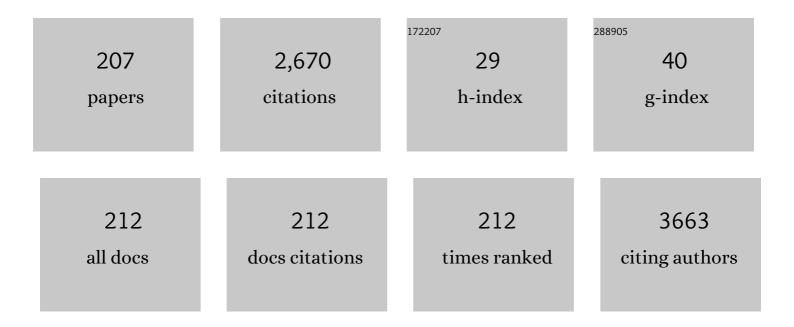
Piotr Dluzewski

List of Publications by Year in descending order

Source: https://exaly.com/author-pdf/4384552/publications.pdf Version: 2024-02-01



PIOTO DI LIZEWISKI

#	Article	IF	CITATIONS
1	Removal of cationic dyes from aqueous solutions using N-benzyl-O-carboxymethylchitosan magnetic nanoparticles. Chemical Engineering Journal, 2012, 183, 284-293.	6.6	92
2	Magnetic properties ofLa0.67Sr0.33MnO3/YBa2Cu3O7superlattices. Physical Review B, 2004, 69, .	1.1	91
3	High-pressure, high-temperature synthesis of SiC–diamond nanocrystalline ceramics. Applied Physics Letters, 2000, 77, 954.	1.5	76
4	Influence of substrate nitridation temperature on epitaxial alignment of GaN nanowires to Si(111) substrate. Nanotechnology, 2013, 24, 035703.	1.3	74
5	ZnTe nanowires grown on GaAs(100) substrates by molecular beam epitaxy. Applied Physics Letters, 2006, 89, 133114.	1.5	71
6	Catalytic growth of ZnTe nanowires by molecular beam epitaxy: structural studies. Nanotechnology, 2007, 18, 475606.	1.3	55
7	Structural and optical properties of low-temperature ZnO films grown by atomic layer deposition with diethylzinc and water precursors. Journal of Crystal Growth, 2009, 311, 1096-1101.	0.7	54
8	TEM study of chirality in MoS ₂ nanotubes. Journal of Microscopy, 1996, 181, 68-71.	0.8	48
9	GaAs:Mn Nanowires Grown by Molecular Beam Epitaxy of (Ga,Mn)As at MnAs Segregation Conditions. Nano Letters, 2007, 7, 2724-2728.	4.5	47
10	Adsorption of Remazol Red 198 onto magnetic N-lauryl chitosan particles: equilibrium, kinetics, reuse and factorial design. Environmental Science and Pollution Research, 2012, 19, 1594-1604.	2.7	45
11	Homogeneous and heterogeneous magnetism in (Zn,Co)O: From a random antiferromagnet to a dipolar superferromagnet by changing the growth temperature. Physical Review B, 2013, 88, .	1.1	43
12	Structural and optical evidence of island correlation in CdTe/ZnTe superlattices. Applied Physics Letters, 2001, 78, 3884-3886.	1.5	42
13	Fluence thresholds for grazing incidence hard x-ray mirrors. Applied Physics Letters, 2015, 106, .	1.5	41
14	Adsorption of Cr(VI) on crosslinked chitosan–Fe(III) complex in fixed-bed systems. Journal of Water Process Engineering, 2015, 7, 141-152.	2.6	41
15	Synthesis, characterization and in vitro drug release of magnetic N-benzyl-O-carboxymethylchitosan nanoparticles loaded with indomethacin. Acta Biomaterialia, 2011, 7, 3078-3085.	4.1	40
16	Lattice parameters and orthorhombic distortion of CaMnO ₃ . Powder Diffraction, 2010, 25, 46-59.	0.4	39
17	Microstructural magnetic phases in superconducting FeTe0.65Se0.35. Superconductor Science and Technology, 2012, 25, 065019.	1.8	39
18	A magnetic nanogel based on O-carboxymethylchitosan for antitumor drug delivery: synthesis, characterization and in vitro drug release. Soft Matter, 2014, 10, 3441.	1.2	39

#	Article	IF	CITATIONS
19	When Eutectics Meet Plasmonics: Nanoplasmonic, Volumetric, Selfâ€Organized, Silverâ€Based Eutectic. Advanced Optical Materials, 2015, 3, 381-389.	3.6	38
20	Preparation, characterization, and application of magnetic activated carbon from termite feces for the adsorption of Cr(VI) from aqueous solutions. Powder Technology, 2019, 354, 432-441.	2.1	37
21	Synthesis of core–shell silver–platinum nanoparticles, improving shell integrity. Colloids and Surfaces A: Physicochemical and Engineering Aspects, 2014, 441, 178-183.	2.3	36
22	Formation and electrochemical properties of composites of the C60–Pd polymer and multi-wall carbon nanotubes. Electrochimica Acta, 2009, 54, 5621-5628.	2.6	35
23	Characterization of dielectric layers grown at low temperature by atomic layer deposition. Thin Solid Films, 2015, 577, 97-102.	0.8	35
24	Hole Trapping Process and Highly Sensitive Ratiometric Thermometry over a Wide Temperature Range in Pr ³⁺ -Doped Na ₂ La ₂ Ti ₃ O ₁₀ Layered Perovskite Microcrystals. Journal of Physical Chemistry A, 2019, 123, 4021-4033.	1.1	35
25	Magnetic Fe doped ZnO nanofibers obtained by electrospinning. Journal of Sol-Gel Science and Technology, 2012, 61, 494-500.	1.1	34
26	Facile synthesis of core/shell ZnO/ZnS nanofibers by electrospinning and gas-phase sulfidation for biosensor applications. Physical Chemistry Chemical Physics, 2015, 17, 24029-24037.	1.3	33
27	Properties of Pd nanocrystals prepared by PVD method. Vacuum, 2007, 82, 372-376.	1.6	32
28	Abundant Acceptor Emission from Nitrogen-Doped ZnO Films Prepared by Atomic Layer Deposition under Oxygen-Rich Conditions. ACS Applied Materials & amp; Interfaces, 2017, 9, 26143-26150.	4.0	32
29	The role of Ca2+ ions in the formation of high optical quality Cr4+,Ca:YAG ceramics. Journal of the European Ceramic Society, 2019, 39, 3344-3352.	2.8	32
30	Kinetics of Cr3+ to Cr4+ ion valence transformations and intra-lattice cation exchange of Cr4+ in Cr,Ca:YAG ceramics used as laser gain and passive Q-switching media. Journal of Chemical Physics, 2019, 151, 134708.	1.2	26
31	MBE Growth and Properties of ZnTe- and CdTe-Based Nanowires. Journal of the Korean Physical Society, 2008, 53, 3055-3063.	0.3	26
32	High temperature magnetic order in zinc sulfide doped with copper. Journal of Physics and Chemistry of Solids, 2011, 72, 648-652.	1.9	25
33	display="inline"> <mml:msub> <mml:mrow></mml:mrow> <mml:mi>x</mml:mi> </mml:msub> Fe <mml:math xmlns:mml="http://www.w3.org/1998/Math/MathML" display="inline"> <mml:msub> /> <mml:mrow> <mml:mn>2</mml:mn> <mml:mo> ^^ </mml:mo> <mml:mi> y</mml:mi> </mml:mrow> xmlns:mml="http://www.w3.org/1998/Math/MathML" display="inline"> <mml:msub> <mml:mrow> <td>ı> <1∺1ml:m</td><td>ath>Se<mm< td=""></mm<></td></mml:mrow></mml:msub></mml:msub></mml:math 	ı> < 1∺1 ml:m	ath>Se <mm< td=""></mm<>
34	/> <mml:mn>2</mml:mn> : Impa. Physical Review B, 2012, 86, . Influence of Cr doping on the phase composition of Cr,Ca: <scp>YAG</scp> ceramics by solid state reaction sintering. Journal of the American Ceramic Society, 2019, 102, 2104-2115.	1.9	24
35	Homogenous indium distribution in InGaN/GaN laser active structure grown by LP-MOCVD on bulk GaN crystal revealed by transmission electron microscopy and x-ray diffraction. Nanotechnology, 2007, 18, 465707.	1.3	23
36	Structure and magnetic characterization of La0.67Sr0.33MnO3/YBa2Cu3O7 superlattices. Journal of Applied Physics, 2004, 95, 2906-2911.	1.1	22

#	Article	IF	CITATIONS
37	Ultra-fast growth of the monocrystalline zinc oxide nanorods from the aqueous solution. International Journal of Nanotechnology, 2014, 11, 758.	0.1	22
38	On the measurement of dislocation core distributions in a GaAs/ZnTe/CdTe heterostructure by high-resolution transmission electron microscopy. Philosophical Magazine, 2003, 83, 231-244.	0.7	21
39	Interplay of superconductivity and ferromagnetism in YBa2Cu3O7/ La1â^'xSrxMnO3 heterostructures. Superconductor Science and Technology, 2006, 19, S38-S44.	1.8	21
40	Electron emissive properties of CNT films grown by catalytic method on different types of substrates. Diamond and Related Materials, 2004, 13, 1008-1011.	1.8	20
41	Morphology and strain of self-assembled semipolar GaN quantum dots in (112Â ⁻ 2) AlN. Journal of Applied Physics, 2010, 108, .	1.1	20
42	Epitaxial Zinc-Blende CdTe Antidots in Rock-Salt PbTe Semiconductor Thermoelectric Matrix. Crystal Growth and Design, 2011, 11, 4794-4801.	1.4	20
43	The growth kinetics of colloidal ZnO nanoparticles in alcohols. Journal of Sol-Gel Science and Technology, 2012, 61, 197-205.	1.1	20
44	Growth conditions and structural properties of ZnMgO nanocolumns on Si(111). Journal of Crystal Growth, 2014, 408, 102-106.	0.7	20
45	Adsorption of the dye Remazol Red 198 (RR198) by O-carboxymethylchitosan-N-lauryl/γ-Fe2O3 magnetic nanoparticles. Arabian Journal of Chemistry, 2019, 12, 3444-3453.	2.3	20
46	Measurement of dislocation core distribution by digital processing of high-resolution transmission electron microscopy micrographs: a new technique for studying defects. Journal of Physics Condensed Matter, 2000, 12, 10313-10318.	0.7	19
47	Zn _{1â^'<i>x</i>} Mn _{<i>x</i>} Te Diluted Magnetic Semiconductor Nanowires Grown by Molecular Beam Epitaxy. Nano Letters, 2008, 8, 4061-4065.	4.5	19
48	Properties of Pd–C films for hydrogen storage applications. Physica Status Solidi C: Current Topics in Solid State Physics, 2011, 8, 2527-2531.	0.8	19
49	On the binding energy of the 12l̂»C(g.s.) hypernucleus. Nuclear Physics A, 1988, 484, 520-524.	0.6	18
50	Self-organized MnAs quantum dots formed during annealing of GaMnAs under arsenic capping. Applied Physics Letters, 2005, 87, 263114.	1.5	18
51	Defect Free PbTe Nanowires Grown by Molecular Beam Epitaxy on GaAs(111)B Substrates. Crystal Growth and Design, 2010, 10, 109-113.	1.4	18
52	Impact of substrate temperature on magnetic properties of plasma-assisted molecular beam epitaxy grown (Ga,Mn)N. Journal of Alloys and Compounds, 2018, 747, 946-959.	2.8	18
53	Dual-acceptor doped <i>p</i> -ZnO:(As,Sb)/ <i>n</i> -GaN heterojunctions grown by PA-MBE as a spectrum selective ultraviolet photodetector. Physica Status Solidi (A) Applications and Materials Science, 2014, 211, 2072-2077.	0.8	17
54	Backscattering analysis of short period ZnO/MgO superlattices. Surface and Coatings Technology, 2018, 355, 45-49.	2.2	17

#	Article	IF	CITATIONS
55	Anisotropic misfit strain relaxation in lattice mismatched InGaAs/GaAs heterostructures grown by MOVPE. Journal of Crystal Growth, 2008, 310, 3014-3018.	0.7	16
56	Transmission electron microscopy studies of the Pd–C films obtained by physical and chemical vapor deposition. International Journal of Hydrogen Energy, 2012, 37, 18556-18562.	3.8	16
57	Light- and environment-sensitive electrospun ZnO nanofibers. RSC Advances, 2013, 3, 5656.	1.7	16
58	Atomic layer deposited ZnO films implanted with Yb: The influence of Yb location on optical and electrical properties. Thin Solid Films, 2017, 643, 7-15.	0.8	16
59	X-ray absorption studies of Fe-based nanocrystalline alloys. Journal of Alloys and Compounds, 2001, 328, 57-63.	2.8	15
60	Growth and Structural Characterization of Zinc Blende HgS. Physica Status Solidi (B): Basic Research, 2002, 229, 73-77.	0.7	15
61	TEM characterization of VLSâ€grown ZnTe nanowires. Physica Status Solidi C: Current Topics in Solid State Physics, 2008, 5, 3780-3784.	0.8	15
62	The source of room temperature ferromagnetism in granular GaMnAs layers with zinc blende clusters. Physica Status Solidi - Rapid Research Letters, 2011, 5, 62-64.	1.2	15
63	Properties of ZnO/ZnMgO nanostructures grown on r-plane Al2O3 substrates by molecular beam epitaxy. Journal of Alloys and Compounds, 2015, 650, 256-261.	2.8	15
64	Role of heat accumulation in the multi-shot damage of silicon irradiated with femtosecond XUV pulses at a 1 MHz repetition rate. Optics Express, 2016, 24, 15468.	1.7	15
65	Amorphous FeCrNi/a-C:H coatings with self-organizednanotubular structure. Scripta Materialia, 2017, 136, 24-28.	2.6	15
66	Ultra-fast epitaxial growth of ZnO nano/microrods on a GaN substrate, using the microwave-assisted hydrothermal method. Materials Chemistry and Physics, 2018, 205, 16-22.	2.0	14
67	Potassium-Promoted Carbon-Based Iron Catalyst for Ammonia Synthesis. Effect of Fe Dispersion. Catalysis Letters, 2002, 81, 213-218.	1.4	12
68	Eugenia umbelliflora mediated reduction of silver nanoparticles incorporated into O-carboxymethylchitosan/y-Fe2O3: Synthesis, antimicrobial activity and toxicity. International Journal of Biological Macromolecules, 2020, 155, 614-624.	3.6	12
69	Atomic force microscopy and transmission electron microscopy investigations of catalytic formed nanotubes in C60/C70+Ni layers. Applied Surface Science, 1999, 141, 350-356.	3.1	11
70	EXAFS analysis of grain boundaries in nanocrystalline Fe85Zr7B6Cu2 alloys. Journal of Alloys and Compounds, 1999, 286, 103-107.	2.8	11
71	Electron emission from C[sub 60]/C[sub 70]+Pd films containing Pd nanocrystals. Journal of Vacuum Science & Technology an Official Journal of the American Vacuum Society B, Microelectronics Processing and Phenomena, 2000, 18, 1064.	1.6	11
72	From fullerenes to carbon nanotubes by Ni catalysis. Diamond and Related Materials, 2000, 9, 901-905.	1.8	11

#	Article	IF	CITATIONS
73	Structure characterization and magnetic properties of oxide multilayers Nd0.67Sr0.33MnO3/YBa2Cu3O7. Physica C: Superconductivity and Its Applications, 2003, 387, 40-43.	0.6	11
74	Electron Doping of Ca4Mn3O10Induced by Vanadium Substitution. Chemistry of Materials, 2005, 17, 4852-4857.	3.2	11
75	Nanometer Size Effect on Magnetic Properties of Sm _{0.8} Ca _{0.2} MnO ₃ Nanoparticles. Journal of Physical Chemistry C, 2012, 116, 435-447.	1.5	11
76	Short-Period CdO/MgO Superlattices as Cubic CdMgO Quasi-Alloys. Crystal Growth and Design, 2020, 20, 5466-5472.	1.4	11
77	Photoelectric work function studies of carbonaceous films containing Ni nanocrystals. Thin Solid Films, 2003, 423, 161-168.	0.8	10
78	XAFS studies of the short-range order in Ni nanoparticles embedded in carbonacoues matrix. Journal of Alloys and Compounds, 2009, 484, 896-901.	2.8	10
79	Negative Hall coefficient of ultrathin niobium in Si/Nb/Si trilayers. Physical Review B, 2014, 90, .	1.1	10
80	The Influence of Technological PVD Process Parameters on the Topography, Crystal and Molecular Structure of Nanocomposite Films Containing Palladium Nanograins. Polish Journal of Chemical Technology, 2014, 16, 18-24.	0.3	10
81	Structural investigations of polytypes in Zn1â^xMgxSe by transmission electron microscopy and cathodoluminescence. Journal of Crystal Growth, 1998, 184-185, 1015-1020.	0.7	9
82	Formation of 4H and 8H polytypes in bulk Zn1â^'xMgxSe crystals. Journal of Alloys and Compounds, 1999, 286, 224-235.	2.8	9
83	Fe:C60 bonds and structure analyzed by computational chemistry methods. Journal of Alloys and Compounds, 1999, 286, 297-301.	2.8	9
84	Morphology and electronic properties of carbon nanotubes grown with Fe catalyst. Journal of Materials Research, 2003, 18, 2451-2458.	1.2	9
85	Magnetic properties of nanogranular CoxCu1â^'x structures. Journal of Alloys and Compounds, 2005, 392, 12-19.	2.8	9
86	Zn _{1â^'<i>x</i>} Mg _{<i>x</i>} Te nanowires grown by solid source molecular beam epitaxy. Nanotechnology, 2008, 19, 365606.	1.3	9
87	Structural and magnetic properties of the molecular beam epitaxy grown MnSb layers on GaAs substrates. Journal of Applied Physics, 2009, 106, .	1.1	9
88	Influence of the Si cap layer on the SiGe islands morphology. Micron, 2009, 40, 122-125.	1.1	9
89	Collective magnetic behavior of biocompatible systems of maghemite particles coated with functional polymer shells. Journal of Magnetism and Magnetic Materials, 2015, 379, 28-38.	1.0	9
90	Synthesis of Ag@Fe2O3 nanocomposite based on O-carboxymethylchitosan with antimicrobial activity. International Journal of Biological Macromolecules, 2018, 107, 42-51.	3.6	9

#	Article	IF	CITATIONS
91	Alkane isomerization on highly reduced Pd/Al2O3 catalysts. The crucial role of Pd-Al species. Catalysis Communications, 2019, 123, 17-22.	1.6	9
92	Characterisation of thin films containing Au and Pd nanoparticles by grazing-incidence X-ray diffraction and related methods. Journal of Alloys and Compounds, 2001, 328, 248-252.	2.8	8
93	Temperature-induced magnetic-anisotropy crossover in a Co/MgO/Co heterostructure. Journal of Applied Physics, 2009, 105, .	1.1	8
94	Nanoindentation of heterogeneous carbonaceous films containing Ni nano-crystals. Micron, 2009, 40, 94-98.	1.1	8
95	Structural and magnetic properties of nanoclusters in GaMnAs granular layers. Journal of Solid State Chemistry, 2011, 184, 1530-1539.	1.4	8
96	Tem and CL Investigations of Pd Nanograins Included in Carbonaceous Film. Solid State Phenomena, 2012, 186, 177-181.	0.3	8
97	Structural investigation of ultrathin Pt/Co/Pt trilayer films under EUV irradiation. Nuclear Instruments & Methods in Physics Research B, 2015, 364, 33-39.	0.6	8
98	Effect of microwave radiation on the adsorption of the dye Remazol Red 198 (RR198) by O-carboxymethylchitosan-N-lauryl/F2O3 magnetic nanoparticles. Chemical Engineering Research and Design, 2016, 102, 392-402.	2.7	8
99	Adsorption of reactive red dye (RR-120) on nanoadsorbent O-carboxymethylchitosan/î³-Fe ₂ O ₃ : kinetic, equilibrium and factorial design studies. RSC Advances, 2016, 6, 35058-35070.	1.7	8
100	Preparation and properties of carbon-palladium multilayer for hydrogen detection. Vacuum, 2016, 128, 265-271.	1.6	8
101	Kesterite Inorganic-Organic Heterojunction for Solution Processable Solar Cells. Electrochimica Acta, 2016, 201, 78-85.	2.6	8
102	Structural Quality and Magnetotransport Properties of Epitaxial Layers of the (Ga,Mn)(Bi,As) Dilute Magnetic Semiconductor. Materials, 2020, 13, 5507.	1.3	8
103	Improved-sensitivity integral SQUID magnetometry of (Ga,Mn)N thin films in proximity to Mg-doped GaN. Journal of Alloys and Compounds, 2021, 868, 159119.	2.8	8
104	TEM characterization of MBE grown CdTe/ZnTe axial nanowires. Journal of Microscopy, 2010, 237, 337-340.	0.8	7
105	Devitrification of thin film Cu–Zr metallic glass via ultrashort pulsed laser annealing. Journal of Alloys and Compounds, 2021, 887, 161437.	2.8	7
106	Do We Understand Magnetic Properties of ZnMnO?. Acta Physica Polonica A, 2007, 112, 261-267.	0.2	7
107	The formation of fullerenes and nanotubules. Journal of Materials Research, 1993, 8, 118-122.	1.2	7
108	Studies of structural changes in layers annealed under oxidative conditions. Vacuum, 1997, 48, 357-361.	1.6	6

#	Article	IF	CITATIONS
109	Topography and structure of C60/C70+Ni film containing carbon nanotubes grown perpendicularly to the substrate. Vacuum, 1999, 54, 57-62.	1.6	6
110	Characterisation of cold electron emitting carbonaceous films containing Ni metallic nanocrystals. Diamond and Related Materials, 2002, 11, 809-812.	1.8	6
111	TEM determination of directions of (Ga,Mn)As nanowires grown by MBE on GaAs(001) substrates. Journal of Microscopy, 2009, 236, 115-118.	0.8	6
112	Magnetic properties of MnAs nanocrystals embedded in GaAs. Journal of Magnetism and Magnetic Materials, 2009, 321, 2788-2791.	1.0	6
113	Structural and magnetic properties of GaAs:(Mn,Ga)As granular layers. Physica Status Solidi (B): Basic Research, 2011, 248, 1609-1614.	0.7	6
114	Magnetic anisotropy of La0.7Sr0.3MnO3 nanopowders. Journal of Magnetism and Magnetic Materials, 2013, 335, 11-16.	1.0	6
115	Spin-current mediated exchange coupling in MgO-based magnetic tunnel junctions. Physical Review B, 2021, 103, .	1.1	6
116	Study of Spin Pumping through αâ€&n Thin Films. Physica Status Solidi - Rapid Research Letters, 2021, 15, 2100137.	1.2	6
117	Structure and Magnetic Characterization οf BiFeO3/YBa2Cu3O7Bilayers. Acta Physica Polonica A, 2009, 115, 95-97.	0.2	6
118	Work function and electron emission from nanocrystalline Pd films. Vacuum, 2001, 63, 355-360.	1.6	5
119	Topographical and morphological studies of the superficial structure changes during the growth of heterogeneous carbonaceous films with Ni nano-crystals inclusion. Vacuum, 2004, 74, 311-315.	1.6	5
120	Platinum Nanoelectrodes Embedded in an Insulating Alumina Matrix: An Innovative Approach. Chemical Vapor Deposition, 2005, 11, 187-190.	1.4	5
121	Structural Characterization of Doped Thick Gainnas Layers - Ambiguities and Challenges. Journal of Electrical Engineering, 2014, 65, 299-303.	0.4	5
122	Synthesis of Bulk Kesterite – A Prospective Photovoltaic Material. European Journal of Inorganic Chemistry, 2014, 2014, 4730-4733.	1.0	5
123	TEM studies on thermally nanocrystallized vanadium-containing glassy analogs of LiFePO4 olivine. Materials Characterization, 2017, 127, 214-221.	1.9	5
124	Self-organized ZnMgO nanocolumns with ZnO/ZnMgO quantum wells on c-plane Al2O3 substrates by MBE: Growth conditions and properties. Journal of Alloys and Compounds, 2018, 737, 748-751.	2.8	5
125	Photoluminescence Properties of ZnO and ZnCdO Nanowires. Acta Physica Polonica A, 2007, 112, 357-362.	0.2	5
126	Coexistance of 2H and 4H polytypes in Zn1â^'xMgxSe observed by photo- and cathodoluminescence. Solid State Communications, 1998, 108, 367-370.	0.9	4

#	Article	IF	CITATIONS
127	Photoelectric work function determination for the nanostructural carbonaceous films. Vacuum, 2003, 70, 237-241.	1.6	4
128	Fabrication and properties of nanocrystalline Znâ€Irâ€O thin films. Physica Status Solidi C: Current Topics in Solid State Physics, 2012, 9, 1504-1506.	0.8	4
129	Formation of two-dimensionally confined superparamagnetic (Mn, Ga)As nanocrystals in high-temperature annealed (Ga, Mn)As/GaAs superlattices. Journal of Physics Condensed Matter, 2013, 25, 196005.	0.7	4
130	Adsorption of CO on various M@Pt core–shell nanoparticles: Surface-enhanced infrared absorption and DFT studies. Vibrational Spectroscopy, 2014, 75, 11-18.	1.2	4
131	Anisotropy of strain relaxation in heterogeneous GalnNAs layers grown by AP-MOVPE. Journal of Crystal Growth, 2015, 430, 14-20.	0.7	4
132	Enhancement of luminescence of nanocrystalline TiO2:Yb3+ nanopowders due to co-doping with Nd3+ ions. Optical Materials, 2015, 47, 361-365.	1.7	4
133	Interface Studies in HgTe/HgCdTe Quantum Wells. Physica Status Solidi (B): Basic Research, 2020, 257, 1900598.	0.7	4
134	Formation and electrochemical properties of multiwalled carbon nanotubes and polypyrrole composite with (n-Oc4N)Br binder. Synthetic Metals, 2021, 272, 116661.	2.1	4
135	Growth and Properties of ZnMnTe Nanowires. Acta Physica Polonica A, 2007, 112, 351-356.	0.2	4
136	Native Deep-Level Defects in MBE-Grown p-Type CdTe. Acta Physica Polonica A, 2011, 120, 946-949.	0.2	4
137	Preparation and Some Properties of Carbon Nanotubes. Acta Physica Polonica A, 1995, 87, 885-891.	0.2	4
138	Study of Zn-related structural transformations at p-GaAs/Ni/Zn interfaces relative to the formation of an ohmic contact. Materials Science in Semiconductor Processing, 2001, 4, 289-291.	1.9	3
139	Structural and magnetic study of Co/Gd multilayers deposited on Si and Si-N substrates. Journal Physics D: Applied Physics, 2001, 34, A208-A213.	1.3	3
140	Photoelectric properties of nanostructured carbonaceous films containing Ni-C nanocrystals investigated by picosecond laser-induced photoelectric charge emission. Diamond and Related Materials, 2004, 13, 1437-1441.	1.8	3
141	ZnSe/CdSe Superlattice Nanowires by Catalyst-assisted Molecular Beam Epitaxy. AlP Conference Proceedings, 2007, , .	0.3	3
142	Dislocation-related electronic states in partially strain-relaxed InGaAs/GaAs heterostructures grown by MOVPE. Physica Status Solidi C: Current Topics in Solid State Physics, 2007, 4, 3037-3042.	0.8	3
143	Misfit dislocations and surface morphology of InGaAs/GaAs heterostructures grown by MOVPE. Physica Status Solidi C: Current Topics in Solid State Physics, 2009, 6, 1918-1921.	0.8	3
144	Extended deep-level defects in MBE-grown p-type CdTe layers. Physica Status Solidi C: Current Topics in Solid State Physics, 2013, 10, 113-116.	0.8	3

#	Article	IF	CITATIONS
145	Structural studies of magnetic Fe doped ZnO nanofibers. Radiation Physics and Chemistry, 2013, 93, 21-24.	1.4	3
146	Synthesis of kesterite nanopowders with bandgap tuning ligands. Crystal Research and Technology, 2015, 50, 743-746.	0.6	3
147	The influence of PVD/CVD processes parameters on Ni catalyst nanoparticles sizes. Journal of Physics: Conference Series, 2018, 1033, 012007.	0.3	3
148	Magnetic and magnetotransport properties of epitaxial La _{0.7} Sr _{0.3} MnO ₃ /SrIrO ₃ /La _{/La_{0.7}Sr_{0.3spin valves. Journal Physics D: Applied Physics, 2018, 51, 385002.}}	ub> Ma nO<:	sub a 3
149	Structural Properties of Co and CoFe Electrodes Forming a Magnetic Tunnel Junction. Acta Physica Polonica A, 2007, 111, 135-140.	0.2	3
150	Nanoscale Morphology of Short-Period {CdO/ZnO} Superlattices Grown by MBE. Crystal Growth and Design, 2022, 22, 1110-1115.	1.4	3
151	On the ordering of Cr1-xAlx alloys (x < 0.33) leading to microprecipitations of X- and β-phases. Crystal Research and Technology, 1985, 20, 655-661.	0.6	2
152	The structural changes of polycrystalline film C ₆₀ /C ₇₀ : Ni caused by Ni diffusion. Journal of Materials Research, 1996, 11, 3146-3151.	1.2	2
153	Electron Emitting Nanostructures of Carbon+Pd System. Molecular Crystals and Liquid Crystals, 2000, 353, 237-242.	0.3	2
154	Transmission electron microscopy and X-ray diffraction studies of Al2CO microcrystals. Materials Chemistry and Physics, 2003, 81, 383-386.	2.0	2
155	Zn[sub 1â^'x]Mn[sub x]Te-based diluted magnetic semiconductor nanowire structures grown by MBE. , 2010, , .		2
156	Ultrathin Niobium in the Si/Nb/Si Trilayers. Acta Physica Polonica A, 2014, 126, A-140-A-144.	0.2	2
157	Structural and magnetic properties of hybrid ferromagnetic metal/semiconductor (ZnTe)/Co core-shell nanowires. Journal of Crystal Growth, 2015, 412, 80-86.	0.7	2
158	Characterization of MgO/TiN bilayer deposited on cube-textured copper using pulsed-laser deposition technique. Thin Solid Films, 2019, 692, 137621.	0.8	2
159	Crystallographic changes in electron pulse annealing of Ti-implanted GaP. Radiation Effects and Defects in Solids, 2020, 175, 719-729.	0.4	2
160	PyHoLo software, a new tool for electron hologram analysis and magnetic investigation. Computer Physics Communications, 2020, 256, 107471.	3.0	2
161	Capacitance Properties of Chemically Prepared Carbon Nanostructure/Polyazulene Composites. ECS Journal of Solid State Science and Technology, 2021, 10, 091017.	0.9	2
162	Structural, magnetostatic, and magnetodynamic studies of Co/Mo-based uncompensated synthetic antiferromagnets. Physical Review Materials, 2019, 3, .	0.9	2

#	Article	IF	CITATIONS
163	Fabrication and Ferroelectric Properties of BiFeO ₃ /BaTiO ₃ Heterostructures. Acta Physica Polonica A, 2016, 130, 511-515.	0.2	2
164	On a computation method for the interpretation of the diffuse scattering from binary solid solutions. Physica Status Solidi A, 1994, 143, 215-222.	1.7	1
165	Transport properties of doped (Sr,Ca)10Cu17O29 single crystals under high hydrostatic pressure. Physica C: Superconductivity and Its Applications, 2000, 338, 291-297.	0.6	1
166	Three-Dimensional Quantum Dot ?Crystal? Formation in CdTe/ZnTe Superlattices. Physica Status Solidi (B): Basic Research, 2002, 229, 445-448.	0.7	1
167	Structure of Magnetically Ordered Si:Mn. Solid State Phenomena, 2007, 131-133, 327-332.	0.3	1
168	Atomic order in magnetic Mn inclusions in Si crystals: XAS and TEM studies. Journal of Non-Crystalline Solids, 2008, 354, 4189-4192.	1.5	1
169	Secondary electron microscopy and transmission electron microscopy studies of carbon nanotubes in C-Ni films. Open Physics, 2011, 9, 344-348.	0.8	1
170	Effects of the annealing temperature on the structural and electronic properties of MBE grown InGaN/GaN quantum wells. Journal of Physics: Conference Series, 2011, 326, 012012.	0.3	1
171	Homogenous and heterogeneous magnetism in (Zn,Co)O. , 2012, , .		1
172	Structural and Chemical Characterization of Al(Ga)N/GaN Quantum Well Structures Grown by Plasma Assisted Molecular Beam Epitaxy. Solid State Phenomena, 2012, 186, 70-73.	0.3	1
173	Structural and magnetic characterization of functional surface coated maghemite nanoparticles. , 2012, , .		1
174	Amorphous - Nanocrystalline Melt Spun Al-Si-Ni Based Alloys Modified with Cu and Zr. Archives of Metallurgy and Materials, 2013, 58, 419-423.	0.6	1
175	Structural and magnetic investigation of single wall carbon nanotube films with iron based nanoparticles inclusions synthesized by CVD technique from ferrocene/ethanol solution. Physica Status Solidi C: Current Topics in Solid State Physics, 2013, 10, 1176-1179.	0.8	1
176	Electric and thermoelectric properties of CdTe/PbTe epitaxial nanocomposite. Functional Materials Letters, 2014, 07, 1440007.	0.7	1
177	C-Pd and C-Pd-Ni films for optical sensing. , 2015, , .		1
178	Study of ultrathin Pt/Co/Pt trilayers modified by nanosecond XUV pulses from laser-driven plasma source. Journal of Alloys and Compounds, 2018, 763, 899-908.	2.8	1
179	High content palladium nanocomposite carbon-palladium films. Journal of Physics: Conference Series, 2018, 1033, 012009.	0.3	1
180	Structural and Chemical Properties of ZnTe Nanowires Grown on GaAs. Springer Proceedings in Physics, 2008, , 233-236.	0.1	1

#	Article	IF	CITATIONS
181	Superconductivity and Magnetism in Nd0.5Sr0.5MnO3/YBa2Cu3O7Superlattices. Acta Physica Polonica A, 2007, 111, 179-183.	0.2	1
182	Magnetoresistance of Si/Nb/Si Trilayers. Acta Physica Polonica A, 2010, 118, 406-408.	0.2	1
183	In Situ Electron Beam Amorphization of Sb ₂ Te ₃ within Single Walled Carbon Nanotubes. Acta Physica Polonica A, 2017, 131, 1324-1328.	0.2	1
184	Properties of GaN Nanocolumns Grown by Plasma - Assisted MBE on Si (111) Substrates. Acta Physica Polonica A, 2011, 120, A-15-A-16.	0.2	1
185	Problems of application of X-ray standing wave technique (XSW) to the study of implanted crystals. , 0, , .		Ο
186	<title>Growth and characterization of Zn1-xMgxSe mixed crystals</title> ., 1997, 3178, 205.		0
187	Magnetoresistive, Mechanically Hard Superlattices of CrN, NbN, TiN Multilayers Deposited on Monocrystalline Si Wafers. Materials Research Society Symposia Proceedings, 2001, 695, 1.	0.1	Ο
188	Electron Doping of Ca4Mn3O10 Induced by Vanadium Substitution ChemInform, 2005, 36, no.	0.1	0
189	<title>Preparation and characterization of Ni<formula><inf><roman>N</roman></inf></formula>
nanocrystals embedded in a carbonaceous matrix</title> . , 2006, , .		0
190	Transport and magnetic characterization of La0.885Sr0.115MnO3/YBa2Cu3O7 superlattices. Physica Status Solidi C: Current Topics in Solid State Physics, 2006, 3, 81-84.	0.8	0
191	<title>Pd nanocrystalline films for electron sources</title> ., 2007, , .		0
192	CdTe Quantum Dots in a Field Effect Structure: Photoluminescence Lineshape Analysis. , 2010, , .		0
193	Optimization of Structure and Magnetic Properties of NdFeBTi Nanocomposite Magnets. Solid State Phenomena, 2012, 186, 206-211.	0.3	Ο
194	Magnetocaloric effect in single crystals of RCoGaO <inf>4</inf> (R = Lu, Yb) layered cobaltites. , 2014, , .		0
195	Properties of Pd nanograins in C-Pd composite films obtained by PVD method. Materials Science-Poland, 2015, 33, 482-487.	0.4	0
196	Magnetic and Structural Study of (ZnTe)/Co Core-Shell Nanowires Grown by Molecular Beam Epitaxy. Acta Physica Polonica A, 2015, 127, 517-519.	0.2	0
197	Eutectics: When Eutectics Meet Plasmonics: Nanoplasmonic, Volumetric, Self-Organized, Silver-Based Eutectic (Advanced Optical Materials 3/2015). Advanced Optical Materials, 2015, 3, 414-414.	3.6	0
198	Strain relaxation induced surface morphology of heterogeneous GaInNAs layers grown on GaAs substrate. Journal of Crystal Growth, 2017, 470, 108-112.	0.7	0

#	Article	IF	CITATIONS
199	Studies of field emission process influence on changes in CNT films with different CNT superficial density. Materials Science-Poland, 2018, 36, 27-33.	0.4	Ο
200	Electron Microscopy and X-ray Structural Investigations of Incommensurate Spin-Ladder Sr _{4.1} Ca _{4.7} Bi _{0.3} Cu ₁₇ O ₂₉ Single Crystals. Acta Physica Polonica A, 2000, 98, 729-737.	0.2	0
201	Magnetism and Superconductivity in Nd0.81Sr0.19MnO3/YBa2Cu3O7Superlattices. Acta Physica Polonica A, 2004, 105, 127-132.	0.2	Ο
202	ZnTe nanowires grown catalytically on GaAs (001) substrates by molecular beam epitaxy. AIP Conference Proceedings, 2007, , .	0.3	0
203	Analysis of atomic structure and structural imperfections of ZnTe and (Zn,Mn)Te nanowires. Acta Crystallographica Section A: Foundations and Advances, 2008, 64, C598-C598.	0.3	0
204	MnAs Nanocrystals Embedded in GaAs. Acta Physica Polonica A, 2008, 114, 1207-1211.	0.2	0
205	Stability and thermal expansion of InN: an X-ray diffraction study. Acta Crystallographica Section A: Foundations and Advances, 2011, 67, C406-C406.	0.3	0
206	Correction to Short-Period CdO/MgO Superlattices as Cubic CdMgO Quasi-Alloys. Crystal Growth and Design, 2020, 20, 7080-7080.	1.4	0
207	Nanostructural Carbonaceous Films With Metal (Pd, Ni) Nanoparticles. NATO Science for Peace and Security Series B: Physics and Biophysics, 2009, , 227-230.	0.2	0